

Para-Selective Cyanation of Arenes by H-Bonded Template

Sandeep Pimparkar,^{a,b,c,†} Trisha Bhattacharya,^{a,‡} Arun Maji,^a Argha Saha,^a Ramasamy Jayarajan,^a Uttam Dutta,^{a,b,c} Gang Lu,^{*d} David W. Lupton^{*b,c} and Debabrata Maiti^{*a,b}

^aDepartment of Chemistry, Indian Institute of Technology Bombay, Powai, Mumbai-400076, India; ^bIITB-Monash Research Academy, near estate office, IIT Bombay, Mumbai. ^cSchool of Chemistry, Monash University, Clayton, VIC 3168, Australia; ^dSchool of Chemistry and Chemical Engineering, Shandong University, Jinan 250100, China.

Supporting Information Placeholder

ABSTRACT: The significance of site selective functionalization stands upon the superior selectivity, easy synthesis and diverse product utility. In this work we demonstrate the *para*-selective introduction of versatile nitrile moiety, enabled by detachable and reusable H-bonded auxiliary. The methodology holds its efficiency irrespective of substrate electronic bias. The conspicuous shift in the step energetics was probed by both experimental and computational mechanistic tools heralds the inception of *para*-deuteration. The synthetic impact of the methodology was highlighted with reusability of directing group and post synthetic modifications.

Site selective C–C bond formation remained a fascinating realm of synthetic methodology owing to its ubiquitous nature in molecular frameworks.¹ Construction of such bonds with the assistance of a directing group has rendered intrinsic electronic and steric bias redundant, providing a generalized tool for positional tunability. Initiated with *ortho*-² functionalizations, template assisted C–H activation of *meta*-^{3–6} position was explored quite recently, while *para* functionalization remains in its infancy. Although exclusive *para*-selective functionalization is prevalent in enzymatic systems,⁷ synthetic recapitulation is limited to a handful of systems. In addition, such transformations are often accompanied by inseparable mixture of regio-isomers. In this regard the assistance of templates can attenuate such encumbrance and allow a broader scope.⁸ However, designing the auxiliary, spanning the larger separation of the hinge point and the *para* position recurs the intrinsic synthetic challenge of directed remote C–H activation and thus remains extremely challenging.⁹

In this context our group has identified and developed 1st generation^{8a} and 2nd generation^{8c} directing templates to allow *para* C–H bond of arenes to be functionalized with superior selectivity and yield. The feasibility of directed *para* functionalization was demonstrated earlier with Pd(II) catalyzed *para*-silylation^{8c} and ketonisation^{8d} employing the nitrile-based biphenyl template. More recently, a Rh(I) catalyzed *para*-C–H olefination was developed.^{8e} Despite different non covalent and electronically assisted approaches for *para*-selective functionalizations⁹ we recently focused on methods by which a *para*-C–H bond can be elaborated to a library of functionally diverse materials. The nitrile group is a versatile motif in synthetic chemistry. Furthermore, nitrile groups alter the molecular properties of the arenes and can be found in the dye industry, agrochemicals and pharmaceuticals. Many nitrile containing pharmaceuticals are in clinical development and over 30 are in the market for various conditions. Classically nitrile or cyanoarenes are generated through substitution or functional group interconversions which either demands harsh reaction condition or involves more than one step

(Figure 1a).¹⁰ Although recent efforts in ligand promoted non-directed cyanation of arenes have been reported (Figure 1b),¹¹ the quest for *para*-selective distal cyanation of arenes remains. In this context, the catalytic synthesis of carbon–nitrile connectivity via C–H activation is mostly restricted to *ortho*- and least pronounced for *meta*-position of arenes.^{12, 13, 14}

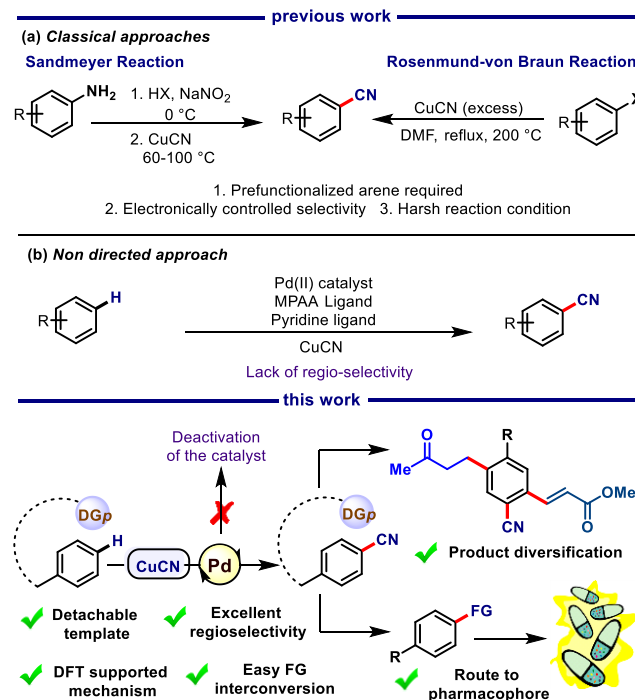
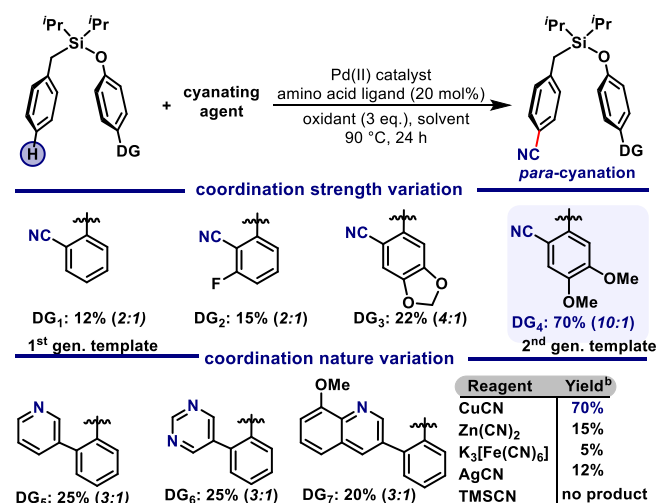


Figure 1. (a) Classical approaches for aryl nitrile synthesis (b) Non directed approach for aryl nitrile synthesis (c) Overview of the present work

Incorporation of a nitrile group under catalytic conditions poses several challenges. Specifically, competition for the binding site of palladium with the directing –CN group and the cyanation source. The strong binding affinity and π -accepting character of nitriles tends to saturate the catalytic site of palladium center leading to deactivation.¹⁵ To overcome the aforementioned problem the choice of solvent is critical as higher solubility of the cyanide ion can exceed the initial concentration of the catalyst leading to catalytic poisoning. Under such circumstances judicious choice of nitrile source with slower release of nitrile can minimize the formation of tetracyanopalladate (II) or palladium (II) cyanide complexes.¹⁶ Systematic understanding and subsequent tuning of reaction parameters led to the development of directed *para* selective cyanation of arenes which overrides electronic and steric

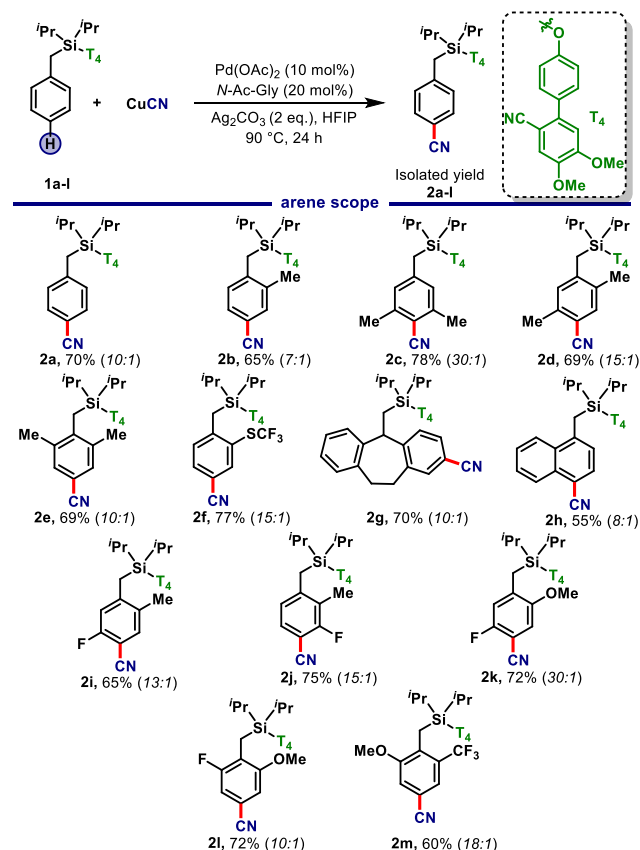
bias using a *para* selective, H-bonding enabled directing template and employing a Pd(II) catalyst.

Scheme 1. Evolution of directing groups and nitrile sources



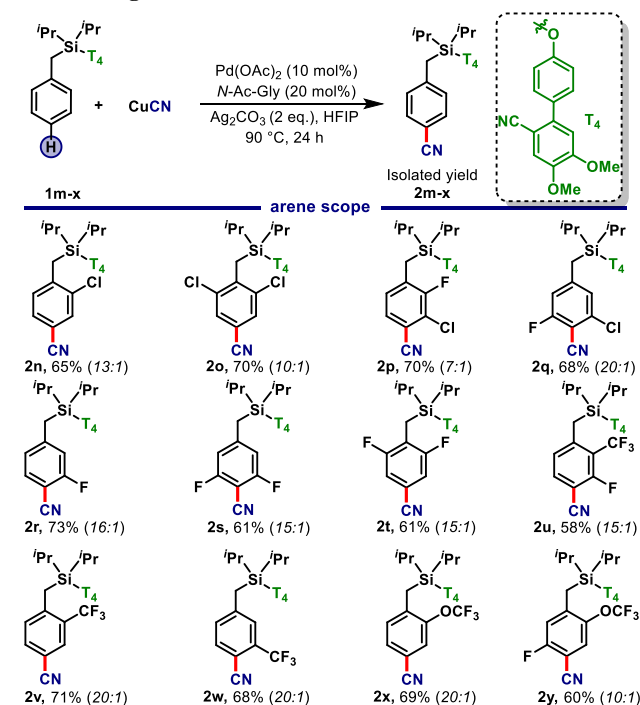
Initially we commenced the cyanation of toluene scaffold using DG₁ (12% yield; *p*: others = 2:1, Scheme 1). Systematic studies of directing templates with strongly coordinating pyridine or quinoline (DG₅-DG₇) improved the yield, yet compromised the selectivity. Modification of the electronic environment around the nitrile group showed further improvements (DG_{2/3/4}). Best output was obtained with dimethoxy substituted template DG₄. Enhanced electron density due to the presence of the dimethoxy group likely improves metal binding and yield while H-bonding interactions with the solvent are likely to provide enhanced structural rigidity to favor specific conformation and necessary superior *para* selectivity. Cuprous cyanide was found to be the most effective nitrile source which might be due to its facile nitrile ligand transfer ability in the rate determining step than any other cyanation sources. After optimizing with DG₄ an overall yield of 70% of cyanation product with 10:1 *para* selectivity was obtained in presence of Pd(OAc)₂ (10 mol%), *N*-Ac-Gly (20 mol%), Ag₂CO₃ (2 eq.) and CuCN (1 eq.) in hexafluoroisopropanol (HFIP) solvent (see supporting information for more information). Upon optimization a range of *para*-cyano toluene derivatives were synthesized with excellent yields and selectivity. Notably the methodology remained unhinged by any electronic and steric inclination of the arene. Toluene derivatives having both electron donating and electron withdrawing substituents (2i-2m) delivered *para* cyano products with comparable yield and selectivity (Table 1). However, substrate 1b bearing an *ortho* methyl group offered a moderate selectivity compared to other substrates. Under the optimized reaction conditions bisarenes fused with a cycloheptane ring possessing two equivalent *para* C-H bonds was selectively converted to the mono cyanated product 2g in 70% yield with good *para* selectivity. Arenes with electron withdrawing substituents were subjected to the established reaction conditions (Table 2). Scaffolds with fluorine at different sites were investigated (2p-u, 2y) due to their medicinal significance. Notably, presence of a highly electron withdrawing trifluoromethyl group could not attenuate the yield or selectivity (2u-2w). A trifluoromethoxy group was also compatible with the current protocol, giving synthetically useful yield and selectivity (2x-y). It is worth to mention that apart from electronic effect -OCF₃ can influence the nature of product formation by distorting its spatial alignment with the benzene ring.

Table 1. Scope of *para*-cyanation on different electron neutral and electron rich toluene scaffolds



All the reactions were carried out using 0.1 mmol of 1, 0.1 mmol of CuCN and 1 mL of HFIP. Yields are of isolated products. Selectivity was determined by ¹H NMR analysis of the crude reaction mixture. The ratios in parentheses are for *para*/others.

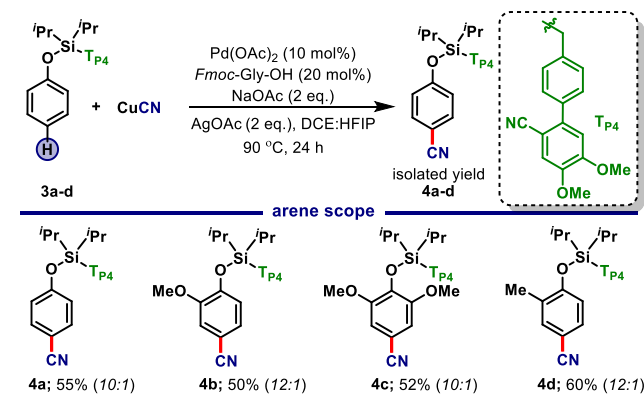
Table 2. Scope of *para*-cyanation on different electron withdrawing toluene scaffolds



All the reactions were carried out using 0.1 mmol of **1**, 0.1 mmol of CuCN and 1 mL of HFIP. Yields are of isolated products. Selectivity was determined by ¹H NMR analysis of the crude reaction mixture. The ratios in parentheses are for *para*/others.

After successful *para*-C–H cyanation of toluene derivatives, we next extended this strategy to other arene systems. To date, C–H activation reactions with phenol derivatives have predominantly occurred at the *ortho* and *meta* positions in the presence of a suitable template, or selectivity has been achieved exclusively based on steric and electronic bias. We reported first *para* selective olefination of phenols in 2016.^{8b} To promote *para* cyanation of phenols we switched the connecting carbon and oxygen atoms in **T**₄ to a modified template **T**_{P4} (Table 3). With the template **T**_{P4} cyanation of phenol substrate **3a** was examined under the established reaction condition for the toluene scaffolds. On our first attempt, the desired cyanated product of phenol was obtained in 30% yield with a 3:1 (*para*:others) selectivity.

Table 3. Scope of *para*-cyanation on different phenol scaffolds

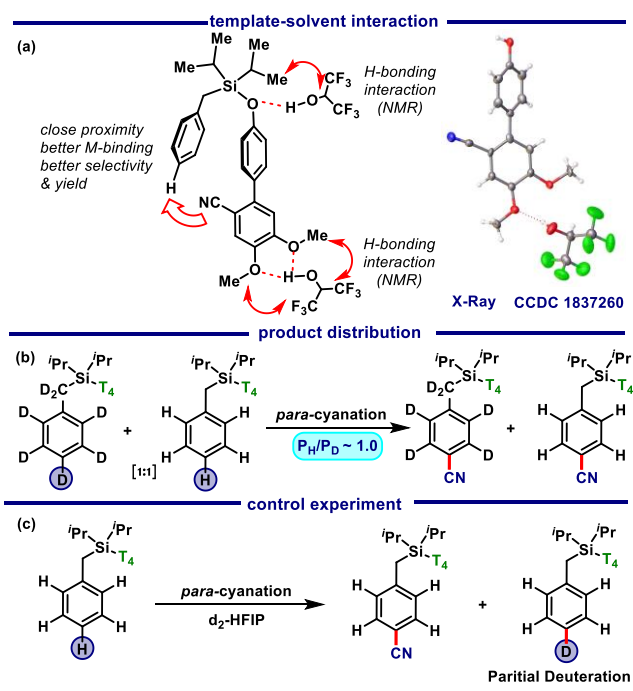


All the reactions were carried out using 0.1 mmol of **3**, 0.1 mmol of CuCN and 1 mL of HFIP. Yields are of isolated products. Selectivity was determined by ¹H NMR analysis of the crude reaction mixture. The ratios in parentheses are for *para*/others.

Subsequently, we optimized other reaction parameters to obtain maximum output. A combination of Pd(OAc)₂ (10 mol%), Fmoc-Gly-OH (20 mol%), AgOAc (2 eq.), NaOAc (2 eq.) and CuCN (1 eq.) in 1:1 mixture of DCE and hexafluoroisopropanol (HFIP) solvent lead to 55% yield and 10:1 *para* selectivity. However, we were unable to elevate the yield of the desired product further and starting material was left unreacted. Phenol derivatives having methoxy (**3b** and **3c**) and *ortho*-methyl substitution (**3d**) allowed formation of cyanated products with moderate yield and greater than 10:1 selectivity.

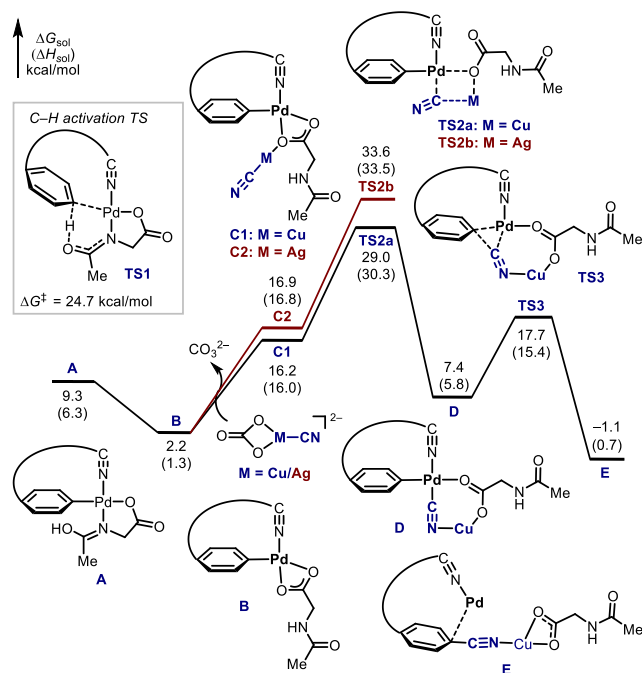
Subsequently we intended to gain better insight into the mechanistic pathway. The crucial role of the solvent HFIP was examined by considering H-bonding interaction between **DG**₄ and the –OH group of HFIP. Evidence for such interactions was provided by NMR titrations (Scheme 2a)^{8c} and also an X-ray crystal structure (CCDC 1837260) reported herewith. Unlike other *para* functionalizations on the same platform, C–H activation step is not associated with the product determining step of the transformation (Scheme 2b) and thus representing reversible C–H activation step. Upon use of d₂-HFIP decreased yield of the desired *para* cyanation product was observed. Most importantly, partially deuterated starting material was recovered which further supports the existence of a reversible C–H activation step (Scheme 2c). We were unable to determine *k*_H/*k*_D value by ¹H NMR analysis due to lack of distinguishable proton peak in the product. Product distribution study was feasible and *P*_H/*P*_D value ~1 further supports a non rate limiting C–H activation pathway.

Scheme 2. (a) Template-solvent interaction (b) Product distribution study (c) Control experiment



The energy profile for the *para* C–H cyanation of substrate **1a** (Scheme 3) was calculated using density functional theory (DFT) and is in agreement with the experimental findings (Scheme 4). Similar to other *para* functionalizations,⁸ the mono-*N*-protected amino acid (MPAA) ligand promotes *para* C–H activation via the CMD mechanism with the *N*-acyl group on the MPAA ligand serving as a base (**TS1** $\Delta G^\ddagger = 24.7$ kcal/mol with respect to separated **1a**, monomeric Pd(OAc)₂ and *N*-Ac-Gly; see details in supporting information). The formed intermediate **A** then tautomerizes and rearranges to the more stable palladacycle **B** with the carboxylic group bound to the Pd center in κ^2 fashion. A series of possible CuCN complexes with anions were also computed. Among these, CuCN(CO₃)²⁻ is the most stable species (see details in supporting information). With respect to CuCN(CO₃)²⁻, the CuCN coordination to the carboxylic group in palladacycle **B** to form **C1** is endothermic by 14.0 kcal/mol. This leads to an overall barrier of 29.0 kcal/mol for the subsequent ligand exchange via a 4-membered σ -bond metathesis transition state (**TS2a**). The resulting palladacycle **D** smoothly undergoes C–C reductive elimination to form the cyanation product. In the overall catalytic cycle, the C–H activation was found reversible, which is consistent with the experimental observation. In addition, the partial solubility of CuCN is critical for the reactivity.¹⁵ Due to the favorable interaction with ^tBuOH ($\Delta G = -7.3$ kcal/mol), CuCN is soluble in ^tBuOH with a relatively high –CN concentration. This increases the possibility of catalyst deactivation, leading to a low yield with ^tBuOH (See Table S7 in Supporting Information). In contrast, the interaction of CuCN with HFIP is thermodynamically neutral ($\Delta G = 0.2$ kcal/mol), which provides the optimum cyanide concentration for the reactivity rather than catalyst deactivation.

Scheme 3. DFT computed energy profile of *para* C–H cyanation with substrate **1a**



We further investigated the origin of reactivity difference when employing the CuCN and AgCN as cyano source. The computed barrier of rate-determining CN ligand exchange with AgCN (TS2b) is 4.6 kcal/mol higher than that with CuCN (TS2a). This is in agreement with the experimentally observed lower reactivity in the reaction with AgCN (Scheme 1). The distortion/interaction analysis¹⁷ indicates that the interaction between the palladacycle fragment and the MCN (M = Cu or Ag) fragment in transition states is the dominated factor to differentiate the reactivity (Figure 2).

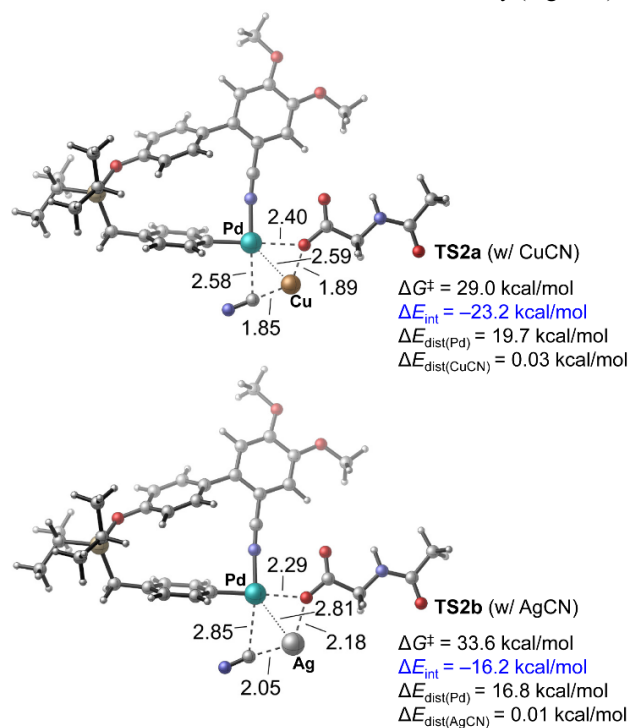
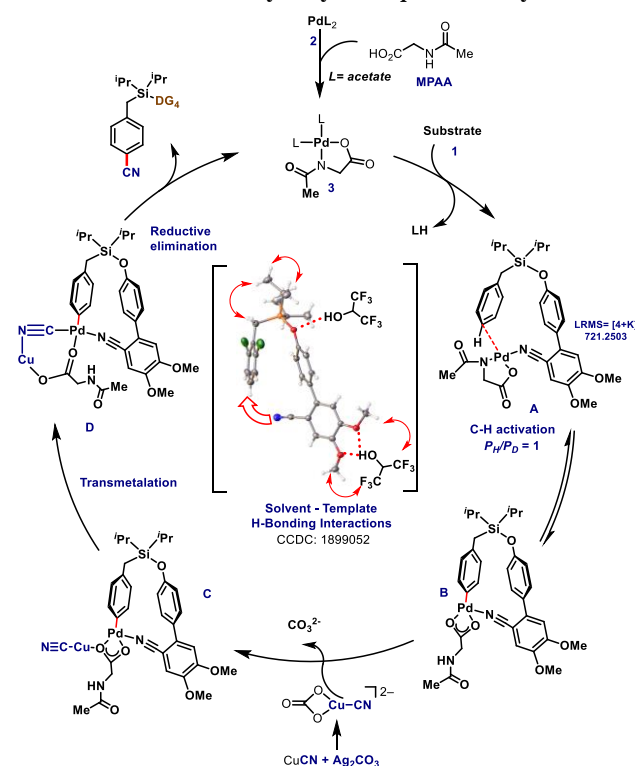


Figure 2. Transmetalation transition states with CuCN and AgCN. Energies are computed at the M06/SDD-6-311+G(d,p)/SMD (HFIP) level of theory with geometries optimized at the

B3LYP/SDD-6-31G(d) level. ΔE_{int} is the interaction energy between the Pd(II) fragment and MCN (M = Cu or Ag) in the transmetalation transition states. Calculated $\Delta E_{\text{dist(Pd)}}$ and $\Delta E_{\text{dist(MCN)}}$ are the energy difference of Pd(II) and MCN fragments between transition states and ground states, respectively.

Compared to the disfavored TS2b with AgCN, the favored TS2a with CuCN shows more favorable interaction energy (ΔE_{int} , Figure 2). This is evidenced by the shorter Pd...Cu and Cu...O distances in TS2a than the Pd...Ag and Ag...O distances in TS2b. The results reveal that the effectiveness of CuCN serving as cyano source is mostly because of the favorable interaction between copper and palladacycle which significantly stabilize the transition state of CN ligand exchange.

Scheme 4. Plausible catalytic cycle for *para* C-H cyanation

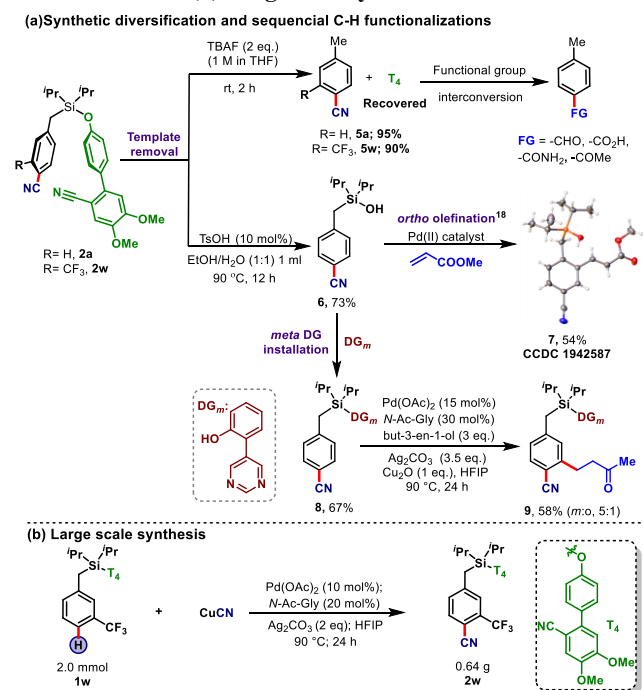


To show the synthetic utility of *para*-cyanated toluenes **2a** and **2w**, at first directing group was removed under ambient condition (Scheme 5a). The directing template **T4** was recovered in quantitative yield along with *para* cyano toluenes (**5a** and **5w**). These aryl nitriles can be transformed to different functional groups and heterocycles. Hydrolysis of **2a** in presence of TsOH gave *para* cyanated silanol **6**, which is a valuable substrate for directed *ortho* functionalization and late stage modifications. The silanol was used as directing group for *ortho* olefination¹⁸ and *meta* alkylation¹⁹ by installing a pyrimidine based directing group. To demonstrate practical efficacy of this protocol the large scale synthesis of **2w** was successfully performed under otherwise identical reaction conditions (Scheme 5b).

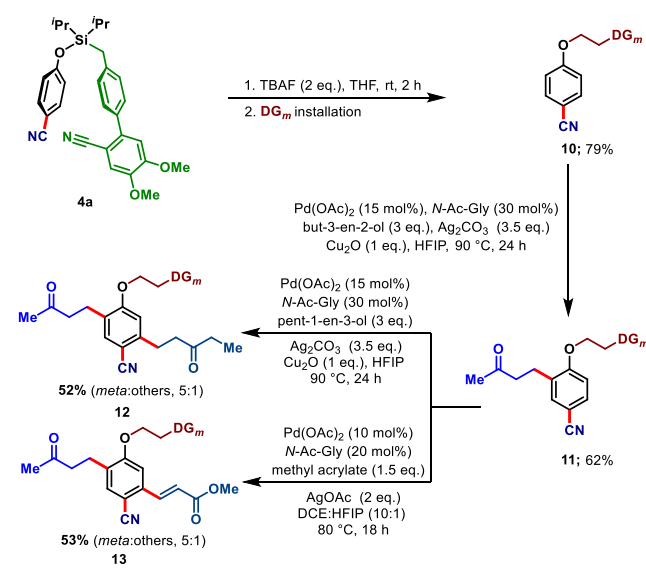
After successful *para* cyanation of phenol, the template was removed *in situ* using TBAF (Scheme 6) and **DG_m** was installed to obtain further C-H functionalized phenols. The strong electron withdrawing influence of the cyano group in **11** led to preferential formation of *ortho* alkylated phenol **12**.¹⁹ Subsequently, this tri-substituted sterically hindered compound **12** was further alkylated and olefinated to obtain *tetra*-substituted arenes **13** and **14**. Such iterative C-H functionalization reactions can demonstrate the

utility of direct protocol without involving functional group interconversions strategies and by avoiding requirement of pre-installation of functional moieties.

Scheme 5. (a) Synthetic diversification and sequential C–H functionalization (b) Large scale synthesis



Scheme 6. Iterative C–H bond functionalization



In summary, we have disclosed a Pd(II) catalyzed H-bonded template assisted *para*-selective cyanation through C–H activation. Discovery of electron rich template allowed us to override the bias present on the aromatic ring. Interestingly C–H activation is not the rate determining step during the cyanation reaction which is further supported by DFT studies. This is in stark contrast with our previous attempts of *para*-C–H functionalization wherein macrocyclic TS for C–H activation was always rate limiting. Distal *para*-C–H cyanation followed by iterative *ortho* and *meta* C–H

bond functionalization demonstrated the utility of direct protocol over traditional functional group interconversions strategy.

ASSOCIATED CONTENT

Supporting Information

The Supporting Information is available free of charge on the ACS Publications Website xxxxx.

AUTHOR INFORMATION

Corresponding Authors

E-mail: D. M.: dmaiti@iitb.ac.in

D. W. L.: david.lupton@monash.edu

Gang Lu: ganglu@sdu.edu.cn

Notes

Authors declare no conflict of interest.

*SP and TB have contributed equally.

ACKNOWLEDGMENT:

This research is supported by SERB (CRG/2018/003951) India. G.L. thanks the financial support from National Natural Science Foundation of China (No. 21973055) and the Natural Science Foundation of Shandong Province (ZR2019MB049). Financial support received from IITB-Monash Research Academy (SP and UD), CSIR-India (AM, AS), UGC (TB) and DST-India (Fast Track Scheme for RJ (YSS/2014/000530).

REFERENCES:

- [1] For general C–C bond formation and C–H activation, see: (a) Murai, S.; Kakiuchi, F.; Sekine, S.; Tanaka, Y.; Kamatani, A.; Sonoda, M.; Chatani, N. Efficient Catalytic Addition of Aromatic Carbon-Hydrogen Bonds to Olefins. *Nature* **1993**, *366*, 529. (b) Kakiuchi, F.; Murai, S. Catalytic C–H/Olefin Coupling. *Acc. Chem. Res.* **2002**, *35*, 826. (c) Seregin, I. V.; Gevorgyan, V. Direct Transition Metal-Catalyzed Functionalization of Heteroaromatic Compounds. *Chem. Soc. Rev.* **2007**, *36*, 1173. (d) Mkhali, I. A. I.; Barnard, J. H.; Marder, T. B.; Murphy, J. M.; Hartwig, J. F. C–H Activation for the Construction of C–B Bonds. *Chem. Rev.* **2010**, *110*, 890. (e) Davies, H. M. L.; Morton, D. Guiding Principles for Site Selective and Stereoselective Intermolecular C–H Functionalization by Donor/Acceptor Rhodium Carbenes. *Chem. Soc. Rev.* **2011**, *40*, 1857. (f) Li, B.-J.; Shi, Z.-J. From C(*sp*²)–H to C(*sp*³)–H: Systematic Studies on Transition Metal-Catalyzed Oxidative C–C Formation. *Chem. Soc. Rev.* **2012**, *41*, 5588. (g) Glorius, F.; Wencel-Delord, J. C–H Bond Activation Enables the Rapid Construction and Late-Stage Diversification of Functional Molecules. *Nat. Chem.* **2013**, *5*, 369. (h) Tobisu, M.; Chatani, N. Remote Control by Steric Effects. *Science* **2014**, *343*, 850. (i) Daugulis, O.; Roane, J.; Tran, L. D. Bidentate, Monoanionic Auxiliary-Directed Functionalization of Carbon–Hydrogen Bonds. *Acc. Chem. Res.* **2015**, *48*, 1053. (j) Gensch, T.; Hopkinson, M. N.; Glorius, F.; Wencel-Delord, J. Mild Metal-Catalyzed C–H Activation: Examples and Concepts. *Chem. Soc. Rev.* **2016**, *45*, 2900. (k) Gemoets, H. P. L.; Kalvet, I.; Nyuchev, A. V.; Erdmann, N.; Hessel, V.; Schoenebeck, F.; Noel, T. Mild and Selective Base-free C–H Arylation of Heteroarenes: Experiment and Computation. *Chem. Sci.* **2017**, *8*, 1046. (l) Parasram, M.; Gevorgyan, V. Silicon-Tethered Strategies for C–H Functionalization Reactions. *Acc. Chem. Res.* **2017**, *50*, 2038. (m) Davies, H. M. L.; Morton, D. Collective Approach to Advancing C–H Functionalization. *ACS Cent. Sci.* **2017**, *3*, 936. (n) Yang, Y.-F.; Hong, X.; Yu, J.-Q.; Houk, K. N. Experimental-Computational Synergy for Selective Pd(II)-Catalyzed C–H Activations of Aryl and Alkyl Groups. *Acc. Chem. Res.* **2017**, *50*, 2853. (o) Shang, R.; Ilies, L.; Nakamura, E. Iron-Catalyzed C–H Bond Activation. *Chem. Rev.* **2017**, *117*, 9086.

- [2] For *ortho*-C–H activation, see: (a) Inoue, S.; Shiota, H.; Fukumoto, Y.; Chatani, N. Ruthenium-Catalyzed Carbonylation at *ortho*-C–H Bonds in Aromatic Amides Leading to Phthalimides: C–H Bond Activation Utilizing a Bidentate System. *J. Am. Chem. Soc.* **2009**, *131*, 6898. (b) Lyons, T. W.; Sanford, M. S. Palladium-Catalyzed Ligand-Directed C–H Functionalization Reactions. *Chem. Rev.* **2010**, *110*, 1147. (c) Patureau, F. W.; Glorius, F. Rh Catalyzed Olefination and Vinylation of Unactivated Acetanilides. *J. Am. Chem. Soc.* **2010**, *132*, 9982. (d) Arockiam, P. B.; Bruneau, C.; Dixneuf, P. H. Ruthenium(II)-Catalyzed C–H Bond Activation and Functionalization. *Chem. Rev.* **2012**, *112*, 5879. (e) Kuhl, N.; Hopkinson, M. N.; Wencel-Delord, J.; Glorius, F. Beyond Directing Groups: Transition-Metal-Catalyzed C–H Activation of Simple Arenes. *Angew. Chem. Int. Ed.* **2012**, *51*, 10236. (f) Dong, Z.; Dong, G. *ortho* vs *ipso*: Site-Selective Pd and Norbornene-Catalyzed Arene C–H Amination Using Aryl Halides. *J. Am. Chem. Soc.* **2013**, *135*, 18350. (g) Haines, B. E.; Musaev, D. G. Factors Impacting the Mechanism of the Mono-*N*-Protected Amino Acid Ligand-Assisted and Directing-Group-Mediated C–H Activation Catalyzed by Pd(II) Complex. *ACS Catal.* **2015**, *5*, 830. (h) Petrone, D. A.; Ye, J.; Lautens, M. Modern Transition-Metal-Catalyzed Carbon–Halogen Bond Formation. *Chem. Rev.* **2016**, *116*, 8003. (i) Li, H. L.; Kuninobu, Y.; Kanai, M. Lewis Acid-Base Interaction-Controlled *Ortho*-Selective C–H Borylation of Aryl Sulfides. *Angew. Chem. Int. Ed.* **2017**, *56*, 1495. (j) Park, Y.; Kim, Y.; Chang, S. Transition Metal-Catalyzed C–H Amination: Scope, Mechanism, and Application. *Chem. Rev.* **2017**, *117*, 9247. (k) Piou, T.; Rovis, T. Electronic and Steric Tuning of a Prototypical Piano Stool Complex: Rh(III) Catalysis for C–H Functionalization. *Acc. Chem. Res.* **2018**, *51*, 170. (l) Li, B.; Seth, K.; Niu, B.; Pan, L.; Yang, H.; Ge, H. Transient Ligand Enabled *ortho*-Arylation of Five Membered Heterocycles: Facile Access to Mechanochromic Materials. *Angew. Chem. Int. Ed.* **2018**, *57*, 3401. (m) Niu, B.; Yang, K.; Lawrence, B.; Ge, H. Transient Ligand-Enabled Transition Metal Catalyzed C–H Functionalization. *ChemSusChem* **2019**, *12*, 2955.
- [3] For selected examples on Pd catalyzed *meta*-C–H functionalization, see: (a) Leow, D.; Li, G.; Mei, T.-S.; Yu, J.-Q. Activation of Remote *meta*-C–H Bonds Assisted by an End-on Template. *Nature* **2012**, *486*, 518. (b) Luo, J.; Preciado, S.; Larrosa, I. Overriding *ortho*–*para* Selectivity via a Traceless Directing Group Relay Strategy: The *Meta*-Selective Arylation of Phenols. *J. Am. Chem. Soc.* **2014**, *136*, 4109. (c) Bera, M.; Maji, A.; Sahoo, S. K.; Maiti, D. Palladium(II)-Catalyzed *meta*-C–H Olefination: Constructing Multisubstituted Arenes through Homo-Diolefination and Sequential Hetero-Diolefination. *Angew. Chem. Int. Ed.* **2015**, *54*, 8515. (d) Wang, X.-C.; Gong, W.; Fang, L.-Z.; Zhu, R.-Y.; Li, S.; Engle, K. M.; Yu, J.-Q. Ligand-Enabled *meta*-C–H Activation Using a Transient Mediator. *Nature* **2015**, *519*, 334. (e) Dong, Z.; Wang, J.; Dong, G. Simple Amine-Directed *meta*-Selective C–H Arylation via Pd/Norbornene Catalysis. *J. Am. Chem. Soc.* **2015**, *137*, 5887. (f) Li, S.; Cai, L.; Ji, H.; Yang, L.; Li, G. Pd(II)-Catalyzed *Meta*-C–H Functionalizations of Benzoic Acid Derivatives. *Nat. Commun.* **2016**, *7*, 10443. (g) Cheng, G.; Wang, P.; Yu, J.-Q. *Meta*-C–H Arylation and Alkylation of Benzylsulfonamide Enabled by a Pd(II)/Isoquinoline Catalyst. *Angew. Chem. Int. Ed.* **2017**, *56*, 8183. (h) Font, M.; Spencer, A. R. A.; Larrosa, I. *Meta*-C–H Arylation of Fluoroarenes via Traceless Directing Group Relay Strategy. *Chem. Sci.* **2018**, *9*, 7133. (i) Li, S.; Wang, H.; Weng, Y.; Li, G. Carboxy Group as a Remote and Selective Chelating Group for C–H Activation of Arenes. *Angew. Chem. Int. Ed.* **2019**, *58*, 18502.
- [4] For selected examples on Ir catalyzed *meta*-C–H functionalization, see: (a) Cho, J.-Y.; Tse, M. K.; Holmes, D.; Maleczka, R. E.; Smith, M. R. Remarkably Selective Iridium Catalysts for the Elaboration of Aromatic C–H Bonds. *Science* **2002**, *295*, 305. (b) Ishiyama, T.; Takagi, J.; Ishida, K.; Miyaura, N.; Anastasi, N. R.; Hartwig, J. F. Mild Iridium-Catalyzed Borylation of Arenes. High Turnover Numbers, Room Temperature Reactions, and Isolation of a Potential Intermediate. *J. Am. Chem. Soc.* **2002**, *124*, 390. (c) Maleczka, R. E., Jr.; Shi, F.; Holmes, D.; Smith, M. R. C–H Activation/Borylation/Oxidation: A One-Pot Unified Route To *meta*-Substituted Phenols Bearing *ortho*–*para*-Directing Groups. *J. Am. Chem. Soc.* **2003**, *125*, 7792. (d) Murphy, J.M., Liao, X.; Hartwig, J. F. *meta* Halogenation of 1,3-Disubstituted Arenes via Iridium-Catalyzed Arene Borylation. *J. Am. Chem. Soc.* **2007**, *129*, 15434. (e) Kuninobu, Y.; Ida, H.; Nishi, M.; Kanai, M. A *meta*-Selective C–H Borylation Directed by a Secondary Interaction between Ligand and Substrate. *Nat. Chem.* **2015**, *7*, 712. (f) Bisht, R.; Chattopadhyay, B. Formal Ir-Catalyzed Ligand-Enabled *ortho* and *meta*-Borylation of Aromatic Aldehydes via in situ-Generated Imines. *J. Am. Chem. Soc.* **2016**, *138*, 84. (g) Davis, H. J.; Mihai, M. T.; Phipps, R. J.; Ion Pair-Directed Regiocontrol in Transition Metal Catalysis: A *Meta*-Selective C–H Borylation of Aromatic Quaternary Ammonium Salts. *J. Am. Chem. Soc.* **2016**, *138*, 12759. (h) Mihai, M. T.; Genov, G. R.; Phipps, R. J. Access to the *meta*-Position of Arenes through Transition Metal Catalyzed C–H Bond Functionalisation: A Focus on Metals other than Palladium. *Chem. Soc. Rev.* **2018**, *47*, 149. (i) Yang, L.; Uemura, N.; Nakao, Y. *Meta*-Selective C–H Borylation of Benzamides and Pyridines by an Iridium–Lewis Acid Bifunctional Catalyst. *J. Am. Chem. Soc.* **2019**, *141*, 7972.
- [5] For selected examples on Ru catalyzed *meta*-C–H functionalization, see: (a) Saidi, O.; Marafie, J.; Ledger, A. E. W.; Liu, P. M.; Mahon, M. F.; Kociok-Köhn, G.; Whittlesey, M. K.; Frost, C. G. Ruthenium-Catalyzed *meta*-Sulfonation of 2-Phenylpyridines. *J. Am. Chem. Soc.* **2011**, *133*, 19298. (b) Teskey, J.; Lui, A.Y.; Greaney, M. F. Ruthenium - Catalyzed *meta*-Selective C–H Bromination. *Angew. Chem. Int. Ed.* **2015**, *54*, 11677. (c) Li, J.; Korvorapun, K.; De Sarkar, S.; Rogge, T.; Burns, D. J.; Warratz, S.; Ackermann, L. Ruthenium(II)-catalyzed Remote C–H Alkylations as a Versatile Platform to *meta*-Decorated Arenes. *Nat. Commun.* **2017**, *8*, 15430. (d) Leitch, J. A.; Frost, C. G. Ruthenium-catalysed σ -activation for Remote *meta*-Selective C–H Functionalisation. *Chem. Soc. Rev.* **2017**, *46*, 7145. (e) Wang, X. G.; Li, Y.; Liu, H. C.; Zhang, B. S.; Gou, X. -Y.; Wang, Q.; Ma, J. -W.; Liang, Y.-M. Three-Component Ruthenium-Catalyzed Direct *Meta*-Selective C–H Activation of Arenes: A New Approach to the Alkylarylation of Alkenes. *J. Am. Chem. Soc.* **2019**, *141*, 13914. (f) Gandeepan, P.; Koeller, J.; Korvorapun, K.; Mohr, J.; Ackermann, L. Visible-Light for Ruthenium-Catalyzed *meta*-C–H Alkylation at Room Temperature. *Angew. Chem. Int. Ed.* **2019**, *58*, 9820. (g) Sagadevan, A.; Greaney, M. F. *Meta*-Selective C–H Activation of Arenes at Room Temperature Using Visible Light Dual-Function Ruthenium Catalysis. *Angew. Chem. Int. Ed.* **2019**, *58*, 9826. (h) Korvorapun, K.; Kuniyil, R.; Ackermann, L. Late-Stage Diversification by Selectivity Switch in *meta*-C–H Activation: Evidence for Singlet Stabilization. *ACS Catal.* **2020**, *10*, 435.
- [6] For selected examples on Rh catalyzed *meta*-C–H functionalization, see: (a) Xu, H.-J.; Lu, Y.; Farmer, M. E.; Wang, H.-W.; Zhao, D.; Kang, Y.-S.; Sun, W.-Y.; Yu, J.-Q. Rh(III)-Catalyzed *meta*-C–H Olefination Directed by a Nitrile Template. *J. Am. Chem. Soc.* **2017**, *139*, 2200. (b) Bera, M.; Agasti, S.; Chowdhury, R.; Mondal, R.; Pal, D.; Maiti, D. XPhos Ligated

Rhodium Catalyzed *meta*-C–H Functionalization of Arenes. *Angew. Chem. Int. Ed.* **2017**, *56*, 5272. (c) Xu, H. –J.; Kang, Y. –S.; Shi, H.; Zhang, P.; Chen, Y. –K.; Zhang, B.; Liu, Z. –Q.; Zhao, J.; Sun, W. –Y.; Yu, J. –Q.; Lu, Y. Rh(III)-Catalyzed *meta*-C–H Alkenylation with Alkynes. *J. Am. Chem. Soc.* **2019**, *141*, 76.

[7] (a) Whited, G. M.; Gibson, D. T. Toluene-4-monooxygenase, a Three-component Enzyme System that Catalyzes the Oxidation of Toluene to *p*-cresol in *Pseudomonas Mendocina* KR1. *J. Bacteriol.* **1991**, *173*, 3010. (b) Fishman, A.; Tao, Y.; Wood, T. K. Toluene 3-monooxygenase of *Ralstonia pickettii* PKO1 is a *para*-Hydroxylating Enzyme. *J. Bacteriol.* **2004**, *186*, 3117.

[8] For selected examples on template assisted *para*-C–H functionalization examples, see: (a) Bag, S.; Patra, T.; Modak, A.; Deb, A.; Maity, S.; Dutta, U.; Dey, A.; Kancherla, R.; Maji, A.; Hazra, A.; Bera, M.; Maiti, D. Remote *para*-C–H Functionalization of Arenes by a D-Shaped Biphenyl Template-Based Assembly. *J. Am. Chem. Soc.* **2015**, *137*, 11888. (b) Patra, T.; Bag, S.; Kancherla, R.; Mondal, A.; Dey, A.; Pimparkar, S.; Agasti, S.; Modak, A.; Maiti, D. Palladium Catalyzed Directed *para*-C–H Functionalization of Phenols. *Angew. Chem. Int. Ed.* **2016**, *55*, 7751. (c) Maji, A.; Guin, S.; Feng, S.; Dahiya, A.; Singh, V. K.; Liu, P.; Maiti, D. Experimental and Computational Exploration of *para*-Selective Silylation with a Hydrogen-Bonded Template. *Angew. Chem. Int. Ed.* **2017**, *56*, 14903. (d) Maji, A.; Dahiya, A.; Lu, G.; Bhattacharya, T.; Liu, P.; Zononi, G.; Maiti, D. H-bonded Reusable Template Assisted *para*-Selective Ketonisation Using Soft Electrophilic Vinyl Ethers. *Nat. Commun.* **2018**, *9*, 3582. (e) Dutta, U.; Maiti, S.; Pimparkar, S.; Maiti, S.; Gahan, L. R.; Krenke, E. H.; Lupton, D. W.; Maiti, D. Rhodium Catalyzed Template-Assisted Distal *para*-C–H Olefination. *Chem. Sci.*, **2019**, *10*, 7426. (f) Li, M.; Shang, M.; Xu, H.; Wang, X.; Dai, H. –X.; Yu, J. –Q. Remote *para*-C–H Acetoxylation of Electron-Deficient Arenes. *Org. Lett.* **2019**, *21*, 540.

[9] For selected examples on diverse *para*-C–H activation, see: (a) Okumura, S.; Tang, S.; Saito, T.; Semba, K.; Sakaki, S.; Nakao, Y. *para*-Selective Alkylation of Benzamides and Aromatic Ketones by Cooperative Nickel/Aluminum Catalysis. *J. Am. Chem. Soc.* **2016**, *138*, 14699. (b) Boursalian, G. B.; Ham, W. S.; Mazzotti, A. R.; Ritter, T. Charge-Transfer-Directed Radical Substitution Enables *para*-Selective C–H Functionalization. *Nat. Chem.* **2016**, *8*, 810. (c) Haines, B. E.; Saito, Y.; Segawa, Y.; Itami, K.; Musaev, D. G. Flexible Reaction Pocket on Bulky Diphosphine–Ir Complex Controls Regioselectivity in *para*-Selective C–H Borylation of Arenes. *ACS Catalysis* **2016**, *6*, 7536. (d) Yang, L.; Semba, K.; Nakao, Y. *para*-Selective C–H Borylation of (Hetero) Arenes by Cooperative Iridium/Aluminum Catalysis. *Angew. Chem. Int. Ed.*, **2017**, *56*, 4853. (e) Leitch, J. A.; McMullin, C. L.; Paterson, A. J.; Mahon, M. F.; Bhonoah, Y.; Frost, C. G. Ruthenium–Catalyzed *para*-Selective C–H Alkylation of Aniline Derivatives. *Angew. Chem. Int. Ed.* **2017**, *56*, 15131. (f) Hoque, E.; Bisht, R.; Haldar, C.; Chattopadhyay, B. Noncovalent Interactions in Ir-Catalyzed C–H Activation: L-Shaped Ligand for *para*-Selective Borylation of Aromatic Esters. *J. Am. Chem. Soc.* **2017**, *139*, 7745. (g) Yuan, C.; Zhu, L.; Chen, C.; Chen, X.; Yang, Y.; Lan, Y.; Zhao, Y. Ruthenium(II)-Enabled *para*-Selective C–H Difluoromethylation of Anilides and Their Derivatives. *Nat. Commun.* **2018**, *9*, 1189. (h) Jiao, Z.; Lim, L. H.; Hirao, H.; Zhou, J. S. Palladium-Catalyzed *para*-Selective Alkylation of Electron-Deficient Arenes. *Angew. Chem. Int. Ed.* **2018**, *57*, 6294. (i) Mihai, M. T.; Williams, B. D.; Phipps, R. J. *Para*-Selective C–H Borylation of Common Arene

Building Blocks Enabled by Ion-Pairing with a Bulky Counteranion. *J. Am. Chem. Soc.* **2019**, *141*, 15477.

[10] (a) Sandmeyer, T. Ber. Ueber die Ersetzung der Amid-gruppe durch Chlor, Brom und Cyan in den aromatischen Substanzen. *Dtsch. Chem. Ges.* **1884**, *17*, 2650. (b) Rosenmund, K. W.; Struck, Das am Ringkohlenstoff gebundene Halogen und sein Ersatz durch andere Substituenten. I. Mitteilung: Ersatz des Halogens durch die Carboxylgruppe. *E. Ber. Dtsch. Chem. Ges. B* **1919**, *52*, 1749. (c) Lindley, J. Tetrahedron Report Number 163 : Copper Assisted Nucleophilic Substitution of Aryl Halogen. *Tetrahedron* **1984**, *40*, 1433.

[11] (a) Chen, H.; Mondal, A.; Wedi, P.; Gemmeren, M. Dual Ligand-Enabled Nondirected C–H Cyanation of Arenes. *ACS Catal.* **2019**, *9*, 1979. (b) Zhao, D.; Xu, P.; Ritter, T. Palladium-Catalyzed Late-Stage Direct Arene Cyanation. *Chem* **2019**, *5*, 97. (c) Liu, L. –Y.; Yeung, K. –S.; Yu, J. –Q. Ligand-Promoted Non-Directed C–H Cyanation of Arenes. *Chem. Eur. J.* **2019**, *25*, 2199.

[12] For concise reviews on arene cyanation reactions, see: (a) Anbarasan, P.; Schareina, T.; Beller, M. Recent Developments and Perspectives in Palladium-Catalyzed Cyanation of Aryl Halides: Synthesis of Benzonitriles. *Chem. Soc. Rev.* **2011**, *40*, 5049. (b) Kim, J.; Kim, H. J.; Chang, S. Synthesis of Aromatic Nitriles Using Nonmetallic Cyano-group Sources. *Angew. Chem., Int. Ed.* **2012**, *51*, 11948. (c) Wen, Q.; Jin, J.; Zhang, L.; Luo, Y.; Lu, P.; Wang, Y. Copper-Mediated Cyanation Reactions. *Tetrahedron Lett.* **2014**, *55*, 1271. (e) Ping, Y.; Ding, Q.; Peng, Y. Advances in C–CN Bond Formation via C–H Bond Activation. *ACS Catal.* **2016**, *6*, 5989.

[13] (a) Sundermeier, M.; Zapf, A.; Mutyala, S.; Baumann, W.; Sans J.; Weiss, S.; Beller, M. Progress in the Palladium–Catalyzed Cyanation of Aryl Chlorides. *Chem. Eur. J.* **2003**, *9*, 1828. (b) Schareina, T.; Zapf, A.; Beller, M. Potassium Hexacyanoferrate(II)—a New Cyanating Agent for the Palladium-Catalyzed Cyanation of Aryl Halides. *Chem. Commun.* **2004**, 1388. (c) Luo, B.; Gao, J. –M.; Lautens, M. Palladium-Catalyzed Norbornene Mediated Tandem Amination/Cyanation Reaction: A Method for the Synthesis of *ortho*-Aminated Benzonitriles. *Org. Lett.* **2016**, *18*, 4166. (d) Hayrapetyan, D.; Rit, R. K.; Kratz, M.; Tschulik, K.; Gooßen, L. J. Electrochemical C–H Cyanation of Electron Rich (Hetero)Arenes. *Chem. Eur. J.* **2018**, *24*, 11288. (e) Wakaki, T.; Sakai, K.; Enomoto, T.; Kondo, M.; Masaoka, S.; Oisaki, K.; Kanai, M. C(*sp*³)-H Cyanation Promoted by Visible-Light Photoredox/Phosphate Hybrid Catalysis. *Chem. Eur. J.* **2018**, *24*, 8051. (f) Yang, L.; Liu, Y. –T.; Park, Y.; Park, S. –W.; Chang, S. Ni-Mediated Generation of “CN” Unit from Formamide and Its Catalysis in the Cyanation Reactions. *ACS Catal.* **2019**, *9*, 3360.

[14] Bag, S.; Jayarajan, R.; Dutta, U.; Chowdhury, R.; Mondal, R.; Maiti, D. Remote *meta*-C – H Cyanation of Arenes Enabled by a Pyrimidine Based Auxiliary. *Angew. Chem. Int. Ed.* **2017**, *56*, 12538.

[15] (a) Erhardt, S.; Grushin, V. V.; Kilpatrick, A. H.; Macgregor, S. A.; Marshall, W. J.; Roe, D. C. Mechanisms of Catalyst Poisoning in Palladium-Catalyzed Cyanation of Haloarenes. Remarkably Facile C–N Bond Activation in the [(Ph₃P)₄Pd]/[Bu₄N]⁺CN[–] System. *J. Am. Chem. Soc.* **2008**, *130*, 4828. (b) Cohen, D. T.; Buchwald, S. L. Mild Palladium-Catalyzed Cyanation of (Hetero)aryl Halides and Triflates in Aqueous Media. *Org. Lett.* **2015**, *17*, 202.

- [16] Takagi, K.; Okamoto, T.; Sakakibara, Y.; Ohno, A.; Oka, S.; Hayama, N. Nucleophilic Displacement Catalyzed by Transition Metal III. Kinetic Investigation of the Cyanation of Iodobenzene Catalyzed by Palladium(II). *Bull. Chem. Soc. Jpn.* **1976**, *49*, 3177.
- [17] Bickelhaupt, F. M.; Houk, K. N., Analyzing Reaction Rates with the Distortion/Interaction-Activation Strain Model. *Angew. Chem. Int. Ed.* **2017**, *56*, 10070.
- [18] Wang, C.; Ge, H. Silanol as a Removable Directing Group for the Pd^{II}-Catalyzed Direct Olefination of Arenes. *Chem. Eur. J.* **2011**, *17*, 14371.
- [19] Jayarajan, R.; Das, J.; Bag, S.; Choudhury, R.; Maiti, D. Diverse *meta*-C-H Functionalization of Arenes across Different Linker Lengths. *Angew. Chem. Int. Ed.* **2018**, *57*, 7659.